EDINBURGH INSTRUMENTS

50 YEARS 1971-2021

RMS1000

RAMAN MICROSCOPE

Extending the capabilities to Photoluminescence Microscopy, Time-Resolved Measurements and Fluorescence Lifetime Imaging (FLIM)

- Truly Confocal
- Five-Position Grating Turrets
- Two Spectrograph Options
- Up to Four Simultaneous Detectors

www.edinst.com

Received: 11 February 2021 | Revised: 17 March 2021 | Accepted: 18 March 2021

DOI: 10.1002/jrs.6105

SPECIAL ISSUE - REVIEW

Journal of RAMAN SPECTROSCOPY WILEY

Detecting rotational disorder in heme proteins: A comparison between resonance Raman spectroscopy, nuclear magnetic resonance, and circular dichroism

Federico Sebastiani[1] | **Lisa Milazzo**[1] | **Cécile Exertier**[2] | **Maurizio Becucci**[1,3] | **Giulietta Smulevich**[1,4]

[1]Dipartimento di Chimica "Ugo Schiff", Università di Firenze, Sesto Fiorentino (FI), Italy

[2]Dipartimento di Scienze Biochimiche "A. Rossi Fanelli", Sapienza, Università di Roma, Rome, Italy

[3]European Laboratory for Non-Linear Spectroscopy–LENS, Sesto Fiorentino (FI), Italy

[4]INSTM Research Unit of Firenze, Sesto Fiorentino (FI), Italy

Correspondence
Giulietta Smulevich, Dipartimento di Chimica "Ugo Schiff", Università di Firenze, Via della Lastruccia 3-13, I-50019. Sesto Fiorentino (Fi), Italy.
Email: giulietta.smulevich@unifi.it

Funding information
MIUR-Italy, Grant/Award Number: Progetto Dipartimenti di Eccellenza 2018-2022; MIUR

Abstract

In heme proteins, the canonical and reversed conformations result from the rotation of the heme group by 180° about the α,γ-meso axis in the protein pocket. The coexistence of the two different heme orientations has been observed both in proteins reconstituted with hemin and in some native proteins. The reversal of the heme orientation can also change certain functional properties of heme proteins. Complementing the results from other experimental techniques, like circular dichroism and nuclear magnetic resonance, resonance Raman spectroscopy provides detailed information on the structure of the reversed heme. This allows one to elucidate the effects of the heme rotation on the vibrational spectra of the peripheral substituents, especially the vinyl groups. Furthermore, the combination of resonance Raman spectroscopy on single crystals and solution samples of heme proteins is proposed to be a sensitive tool to detect heme orientational disorder, even in the absence of structural data.

KEYWORDS

double heme insertion, heme isomerism, heme orientation, reversed heme, vinyl orientation

1 | INTRODUCTION

Heme *b* (iron protoporphyrin IX) is an essential molecule for many living organisms and heme-containing proteins constitute a very important subfamily of metalloproteins, carrying out a high variety of functions, such as oxygen transport, oxygen reduction, electron transfer, catalysis, and gas sensing. All these activities are modulated by the iron atom and regulated by several essential interactions between the heme and the protein surrounding the heme binding site.

The heme prosthetic group is a tetrapyrrole ring, containing a central iron ion (ferric or ferrous), which is bound to the nitrogen atoms of the four pyrrole rings, identified as A, B, C, and D. Moreover, one or two ligands are bound to the axial coordination positions. In many

ABBREVIATIONS: CD, circular dichroism; Hb, hemoglobin; Hb A, human (adult) Hb; *Hs*-Nb, human nitrobindin; Mb, myoglobin; *Mt*-Nb, *Mycobaterium* nitrobindin; Ngb, neuroglobin; NMR, Nuclear Magnetic Resonance; rHb, recombinant Hb; RR, resonance Raman; SW, sperm whale; WT, wild-type.

heme proteins the fifth axial coordination position (proximal side) is occupied by a histidine residue, other possible residues are cysteine, methionine, and tyrosine. The sixth coordination position can be either occupied by an internal ligand or available for binding exogenous ligands. Moreover, heme *b* has four peripheral methyl groups, two vinyl groups, and two propionate side chains, with four methine bridges at the α-δ-*meso* positions on the porphyrin framework. Since the order of linkage of the peripheral methyl and vinyl substituents to the A and B pyrrole rings is asymmetrical, the native heme exists in two possible orientations, resulting from a 180° rotation about the α,γ-*meso* axis in the heme pocket. In the canonical orientation, which represents the most species in native heme proteins, the four peripheral methyl groups are located at the 1, 3, 5, and 8 positions, the two vinyl groups at the 2 and 4 positions, and the two propionate side chains at the 6 and 7 positions. Reconstitution of heme proteins with hemin has been shown to give rise also to a conformer, which differs in the orientation of the heme group by a 180° rotation about the α,γ-*meso* axis in the heme pocket, called reversed heme. In this conformation the order of the two methyl and two vinyl groups at positions 1–4 of the β carbons of the A and B pyrrole rings is changed, the methyl groups being at position 2 and 4, and the two vinyl groups are at the 1 and 3 positions. Figure 1 shows the double heme conformation observed in murine neuroglobin (Ngb).[1–13]

Usually, the amount of reversed heme detected is quite small and its presence depends not only on the specific globin, but also on the oxidation and ligation states of the heme iron. The nature of the ligands has also been shown to be important[1–3,6–8,13–20] and the reversed heme orientation can affect the activity or the functional properties of the proteins.[21–25] For example, it was reported that the two conformer populations of native oxidized myoglobin (Mb) unfold and refold following two parallel kinetic reactions with rate constants differing 10-fold, despite having identical absorption spectra and equilibrium thermodynamic stability.[26] In some bacteria, the reversed heme conformer was shown to a have a stronger selectivity and affinity for the protein matrix than the canonical form upon heme modification, thus becoming a possible antibiotic target.[27,28] Studies on insect heme proteins showed that the amount of reversed conformer is correlated to the physiological function and conserved residues.[29] Moreover, several vertebrate globins, including rainbow trout,[21] sperm whale (SW), equine, bovine and elephant Mb,[2] and the *b* subunits of human hemoglobin (Hb A)[6] were found to contain about 10% of reversed conformer. In particular, the relative amount of reversed heme depends on the heme pocket environment: the hydrophobic interactions between the neighboring apolar residues and the porphyrin ring, along with the preferences for vinyl-protein contacts were shown to be much more important than the salt-bridges between the heme propionate groups and aminoacids.[30] Even the mutation of residues that are not in contact with the heme may affect the kinetics of the heme reorientation and influence the ability of the Mb protein to favor one isomer over the other.[31] The external conditions can also play a role on the rotational isomerism, for example, refolding of the reversed form to a native-like conformation was observed at acidic pH for SWMb.[32]

Unlike other globins, heme structural heterogeneity represents a remarkable feature in neuroglobin (Ngb), a neuroprotective globin present in both vertebrates and invertebrates[33] and predominantly expressed in neurons of the central and peripheral nervous systems.[34] The reversed conformer has a 70% occupancy in murine Ngb as evidenced by Nuclear Magnetic Resonance (NMR)[35] and X-ray diffraction.[4] Therefore, the heme double conformation has been proposed to be responsible not only

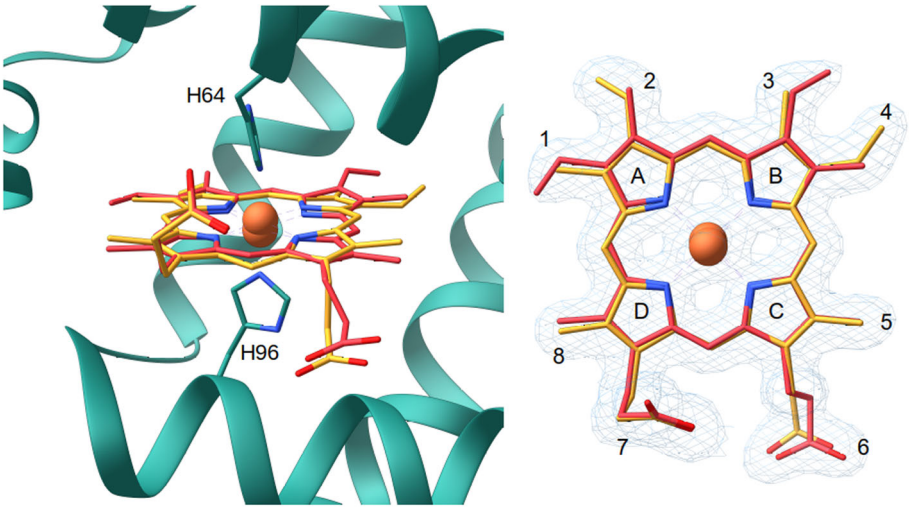

FIGURE 1 Double heme conformation in the hexacoordinated ferric wild-type murine neuroglobin observed by X-ray crystallography (1Q1F). Left: Relative positions of the heme conformations in the heme pocket showing the coordination of His64 (distal) and His96 (proximal) to the heme iron. Right: View of the double heme conformation. In red, the canonical heme orientation, in yellow the reversed heme [Colour figure can be viewed at wileyonlinelibrary.com]

for the effective mechanism of controlling oxygen affinity,[36] but also for the slightly biphasic CO-binding kinetics[5,37] and for cyanide ligation rates.[16]

The heme rotational disorder has been identified through reconstitution studies of wild type and mutant proteins, with both native and a variety of chemically-modified hemes. The studies have been carried out predominantly by the spectroscopic techniques of circular dichroism (CD),[9,18,19,38,39] NMR,[1,2,6–8,10–13,35] and more recently resonance (RR) spectroscopy,[21,40–43] these three techniques providing complementary information.

This review, after a short summary of the results obtained by CD and NMR, will focus on the capability and sensitivity of resonance Raman spectroscopy to give insight into the structure of the reversed heme, elucidating the effects of the heme rotation on the vibrational spectra of the vinyl groups.

2 | CIRCULAR DICHROISM

Free heme is not optically active, and it exhibits a CD signal only when it is incorporated into the chiral environment of the protein internal pocket.[44] It is widely accepted that coupled-oscillator interactions between the $\pi \rightarrow \pi^*$ transitions on the porphyrin and those in the nearby aromatic residues are the origin of this phenomenon. However, this alone cannot account for the observed sensitivity of the relative intensity and the sign of the CD bands to the orientational disorder in heme proteins. In fact, a correlation between reversed heme orientation and negative ellipticity in the near UV and Soret CD spectrum has been established.[9,18–20,25,38,39,45]

In order to explain the fact that monomeric Hb from *Chironomus thummi thummi* (CTTHb) has a negative Soret CD band, while Hbs and Mbs generally exhibit a positive CD band in the Soret region, Woody and Pescitelli estimated that the orientation of the heme vinyl side-chains has a more prominent influence on the Soret CD than the interactions between the $\pi \rightarrow \pi^*$ transitions of the porphyrin and nearby aromatic residues.[46] As the conformation of the heme side chains in CTTHb is similar to that observed in Hb A with the heme in the reversed form, it was speculated that such an orientation influences the Soret CD spectrum of the canonical and reversed isomers.[47] Recently, the combination of CD spectroscopy and time dependent density functional theory analysis, performed on native Mb and Mb reconstituted with synthetic hemes lacking vinyls and/or propionates, has supported this interpretation, but favoring a larger contribution of the propionyl groups with respect to that of the vinyls. In fact, it was shown that up (proximal side) and down (distal side) orientations of the propionates display a positive and negative CD spectrum respectively, and that their corresponding magnitude depends on their position. Moreover, Nagatomo and collaborators demonstrated that the nonplanarity of the heme may also cause a negative Soret CD spectrum, which is significant for the rotational strength of the CD signal.[48]

Therefore, the distinct optical activity of the canonical and reversed heme is due to both the different orientations adopted by the neighboring residue side chains and the difference in planarity existing between the two conformers.[47] As an example, we show in Figure 2 the comparison of the CD spectra obtained for the deoxy form and the CO adducts (inset) of recombinant Hb A (rHb A) and native Hb A.[49] While the native protein contains only the canonical heme form, the recombinant protein exhibits a mixture of canonical and reversed conformers. The bands in the near-UV (L band) and Soret (B band) regions are positive for native Hb A, while distinct changes are observed for the recombinant species. The positive band near 260 nm for the rHb A decreases compared to that of Hb A and, in the Soret region, the protein shows two bands of opposite sign with a relative intensity depending on the coordination state. In fact, for the deoxy species of rHb A, a prominent positive band with a small negative CD band were detected in the Soret region, while for the CO complex of rHb A, the band at 413 nm was prominently negative with a small positive counterpart at 423 nm.

3 | NUCLEAR MAGNETIC RESONANCE

NMR has been considered to be the main tool for detecting and quantifying heme heterogeneity in proteins. In fact, the rotation of the canonical heme by 180° about the α,γ-meso axis yielding the reversed isomer (Figure 1), brings about the exchange of the methyl groups at positions 1 and 3 with the vinyl groups at positions at 4 and 2, respectively, altering the heme methyl and vinyl peripheral contacts with the globin polypeptidic chain. La Mar and coworkers showed that the heme methyl proton signals could be resolved above 13 ppm and that the reversed heme signal is reflected in the heme methyl proton shift. In particular, the α and β subunits of met-azido native HbA give rise to two different sets of heme methyl proton signals, and six extra peaks were observed in the reversed heme NMR profile.[6,7]

Furthermore, the NMR results showed that two conformations with a ratio of 1:1 are detected upon hemin insertion into SW apoMb in the presence of a cyanide ion, indicating that (i) the heme is first bound

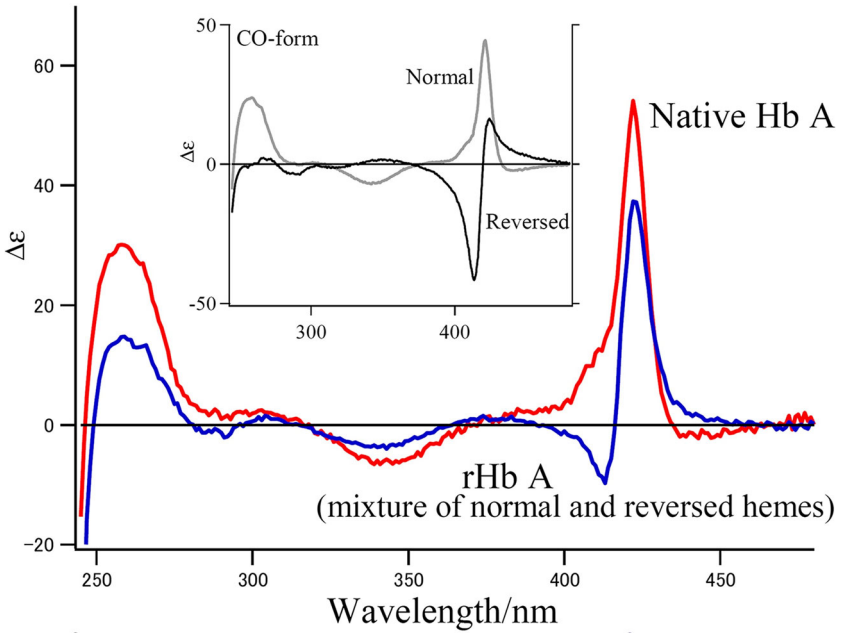

FIGURE 2 CD spectra of deoxy native Hb A (red) and recombinant Hb a (rHb A) (mixture of normal and reversed hemes) (blue). The inset compares the CO adduct of rHb A, (black) and native Hb A (gray). Adapted from Nagai et al.[49] [Colour figure can be viewed at wileyonlinelibrary.com]

non-selectively and (ii) the equilibrium between canonical and reversed conformations is shifted in favor of the canonical conformation over a period of 1 hr.[2] Conversely, Yee et al. observed that for equine Mb, unlike SWMb, hemin reconstitution in the presence of dicyanide displays an increased population of the dominating heme insertion at equilibrium.[50] In fact, the mechanism of heme rotation remains to be further clarified.[3] Time-dependent spectral changes indicate that both the extent of heme rotational disorder and the rate of reorientation depend on the heme peripheral substituents in Mb, horseradish peroxidase (HRP), cytochrome *b5*, and Hb.[6,7,12,50–53] Other studies on Mb reconstituted with artificially modified hemins supported the idea that the contacts of the peripheral substituents, especially the vinyl groups, with the residues of the heme pocket are much more important in determining the preferential heme orientation than the propionate-protein salt bridges.[54] More recently, the crucial role of steric interactions between the residue side chains and the heme peripheral groups in heme binding was identified,[55,56] favoring the intramolecular reorientation mechanism within the Mb heme crevice over the intermolecular mechanism.[56,57]

4 | RESONANCE RAMAN SPECTROSCOPY OF HEME PROTEINS

RR spectroscopy is a very sensitive technique to study biological molecules. In fact, it is non-destructive, it does not require a concentrated sample or a large volume (usually 30–50 μM, 50 μl), water bands are very weak and, therefore, do not interfere with the bands of the sample. Moreover, the development of Raman microscopy, consisting of an optical microscope coupled to a Raman spectrometer,[58] enabled the technique to be applied to the study of heme protein single crystals by using resonance Raman (micro-RR).[59–61]

This technique allows the structural information of the heme pocket obtained by RR in the solution and crystal states to be compared with that from the X-ray structures, to assess the correspondence between the features of the protein under physiological conditions and those in the crystal as determined by X-ray diffraction.[62]

In RR, the vibrational modes of the chromophore can be selectively intensified by the resonance conditions, i.e. by working with a Raman excitation wavelength close to that of an electronic absorption maximum of the target molecule. This characteristic has led to an extensive application of the technique in the study of heme proteins.[63] Therefore, due to the fact that $\pi \rightarrow \pi^*$ electronic transitions of the heme chromophoric group give rise to absorbance maxima at the Soret (380–440 nm) and visible Q bands (500–600 nm),[64] excitation at these wavelengths leads to intense heme vibrational modes enabling identification of core size marker bands (skeletal modes) in the 1300–1700 cm^{-1} region. These modes provide information on the oxidation, coordination and spin states, their wavenumbers being inversely correlated with the size of the porphyrin core.[63–67]

More specifically, laser excitation in the Soret or Q bands regions enhances different sets of Raman bands via different resonance scattering mechanisms. Namely, the totally symmetric modes, which connect the ground

state to the excited state involved in resonance through the Frank-Condon integrals (A term scattering, usually better observed with Soret excitation), and the non-totally symmetric modes via vibronic mixing between the Q band and Soret band (B term scattering, usually better observed with Q band excitation).[63,68]

Furthermore, information on the orientation of the two vinyl groups with respect to the porphyrin macrocycle can be obtained on the basis of the wavenumbers of the vinyl stretching and bending modes.[69–71] When fully conjugated with the porphyrin macrocycle, the two vinyl substituents of heme *b* strongly affect the electronic absorption spectrum (usually a red-shift of up to 10 nm is observed). Consequently, upon Soret excitation, two ν(C=C) stretching modes are observed in the RR spectra of heme *b* proteins[72] and their wavenumbers have been found to range from 1618 to 1635 cm^{-1}. In most heme proteins, two distinct stretching modes have been identified, whereas in a few cases only a single band, deriving from both vinyl groups, has been observed at about 1620 cm^{-1} (e.g., in Mb,[72] cytochrome *b*,[73,74] cytochrome *c* peroxidase (CCP)[70,71]). In 2003, a direct relationship between the ν(C=C) stretching mode wavenumber and the vinyl group orientations induced by specific protein interactions was established.[71] This correlation was based on the combined analysis of X-ray structures, amino acid sequence alignment and spectroscopic data (both electronic absorption and RR spectra) obtained on Mb, several members of the plant peroxidase superfamily, their selected mutants, and their complexes with imidazole and fluoride. In this study Marzocchi and Smulevich showed that (i) the interactions with neighboring residues, resulting from van der Waals contacts, weak π–π electron interactions and C—H· · ·O hydrogen bonds, are responsible for the orientation of the vinyl groups and, therefore, for their specific Raman wavenumbers; (ii) a correlation exists between the ν(C=C) stretching wavenumber and the torsion angle, τ, of a vinyl group formed between the $C_a = C_b$ vinyl double bonds and the $C_\alpha = C_\beta$ of the pyrrole (Figure 3), which determines the vinyl orientation with respect to the porphyrin plane.

As the conjugation between the vinyl double bonds and the porphyrin aromatic macrocycle increases, the ν(C=C) stretching mode wavenumber downshifts. In fact, for the highly conjugated arrangement, that is, the trans vinyl conformation, where the $C_a = C_b$ vinyl double bond is nearly parallel to both the $C_\alpha = C_\beta$ and N_{pyr}—Fe bonds, the ν(C=C) stretching modes were found at about 1618–1620 cm^{-1} (e.g. in Mb, CCP); for the low conjugation arrangement, that is, the cis vinyl conformation, where the $C_a = C_b$ vinyl double bond is nearly orthogonal to both the $C_\alpha = C_\beta$ and N_{pyr}—Fe bonds, the ν(C=C) stretching modes were found at about 1630–1635 cm^{-1} (e.g., HRPC and the alkaline form of CCP); for the twist conformation, which is in between the trans and cis arrangements, the ν(C=C) stretching modes were found at intermediate wavenumbers (e.g. *Arthromyces ramosus*/*Coprinus cinereus* peroxidases). In contrast, the corresponding vinyl bending mode $\delta(C_\beta C_a C_b)$ wavenumber is not strictly correlated with the vinyl orientation.

A similar analytical treatment was tentatively applied to cytochromes P450. Although a corresponding mathematical function, which correlates the wavenumber of the vinyl stretching modes and the torsional angles, as found for peroxidases, apparently is not evident for cytochromes P450, the authors concluded that a similar

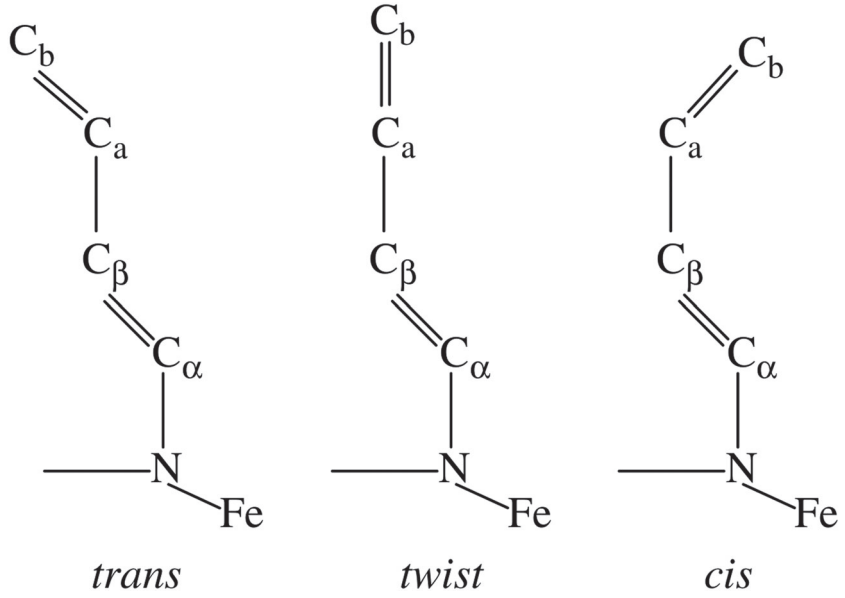

FIGURE 3 Schematic representation of different vinyl conformations as found in heme proteins: Trans (τ = 135°), twist (τ = 90°), cis (τ = 45°). From Marzocchi and Smulevich[71]

relationship may exist.[75] However, the correlation found by Marzocchi and Smulevich was successfully applied to many other heme proteins, such as catalase peroxidase, KatG,[76] a non-symbiotic plant hemoglobin from *Arabidopsis thaliana,*[77] dehaloperoxidase from *Amphitrite ornate,*[78] soluble guanylate cyclase,[79,80] human cytochrome CYP17A1,[81] coproheme (HemQ) from *Staphylococcus aureus*[82] and *Listeria monocytogenes,*[83] truncated hemoglobin (Ph-2/2HbO-2217) from the Antarctic cold-adapted bacterium *Pseudoalteromonas haloplanktis* TAC125,[84] coproporphyrin ferrochelatase,[85] mycobacterial and human Nitrobindins.[86,87] Notably, De Simone and colleagues showed that for both ferric Mycobaterium, *Mt*-Nb, and human nitrobindins, *Hs*-Nb, the theoretical torsion angle predicted for the two vinyls of the heme on the basis of the RR wavenumbers of the vinyl stretching modes closely matched those experimentally measured in the X-ray structure (Figure 4).[86,87]

5 | RR OF THE REVERSED CONFORMATION

In 2008, Kincaid and coworkers undertook a systematic study on reconstituted heme proteins with isotopically labeled protohemes at the peripheral methyl groups by combining NMR and RR spectroscopies, in order to elucidate the specific spectral changes associated with heme orientational disorder.[41] They demonstrated for the first time that RR spectroscopy is a powerful technique to probe such changes. In particular, the data clearly indicated that in both the high (1100–1700 cm^{-1}) and low (150–800 cm^{-1}) wavenumber regions, the modes associated with peripheral vinyl groups, are affected by the heme orientational disorder. The authors demonstrated, by means of NMR, that within 30 min after reconstitution of Mb 35% of the heme is in the reversed form and that only 4% remains in this conformation after 96 hr. Figure 5 shows the NMR spectral changes as a function of time after the reconstitution of Mb with protoheme. After 30 min from reconstitution, a new set of methyl peaks were observed, as predicted by LaMar,[6] whose intensity decreases as a function of time after reconstitution (Figures 5**, traces B–F**). Correlated changes were also observed in the Raman spectra upon reconstitution. The RR spectrum of the reversed conformer of Mb was obtained by comparing the spectra of the native protein to that of the reconstituted sample after 30 minutes, relying on the bands that are either non sensitive or not directly correlated to the rotational disorder. In the low wavenumber region, the comparison with the native protein containing the heme in the canonical orientation clearly showed the presence of new vibrational modes, together with modifications in the relative intensity of some other observed bands. In the high wavenumber region (Figure 6) the most significant differences were observed in the vinyl stretching region.

Unlike the Mb canonical conformation, which shows two overlapped vinyl stretching modes at 1620 cm^{-1},[88] the reversed conformation displays two bands at 1620 and 1630 cm^{-1}, which indicates that the conformation of

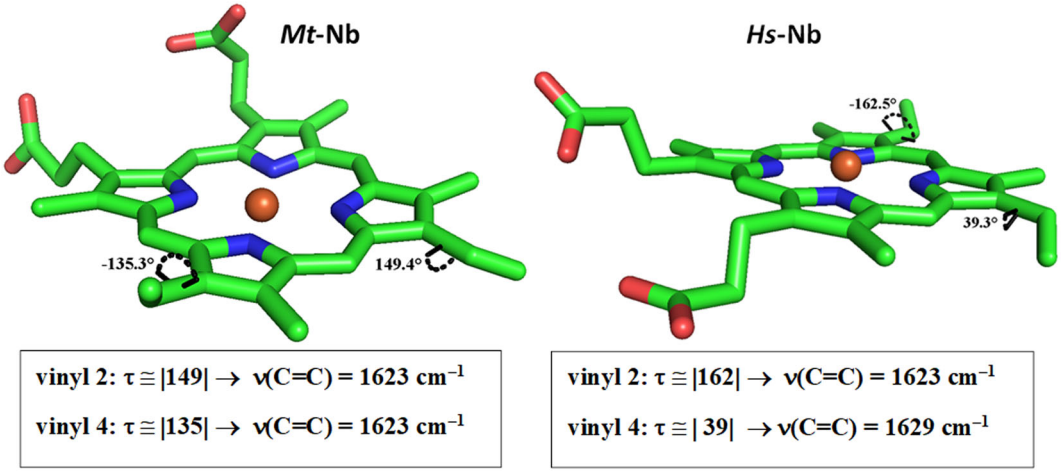

FIGURE 4 Heme cavity structure of *Mt*-Nb (III) (left) (PDB code 2FR2,[81]) and *Hs*-Nb (III) (right) (PDB code: 3IA8,[82]) showing the different conformations of the vinyl groups, measured by the torsional angles (τ) involving the four atoms ($C_\alpha = C_\beta$) and ($C_a = C_b$) of the pyrrole and vinyl double bonds. In the inset, the wavenumbers of the ν(C=C) vinyl stretching modes, indicative of the conjugation and, therefore, correlated to the orientation of the vinyl groups with the porphyrin double bonds ($C_\alpha = C_\beta$). From De Simone et al.[86] [Colour figure can be viewed at wileyonlinelibrary.com]

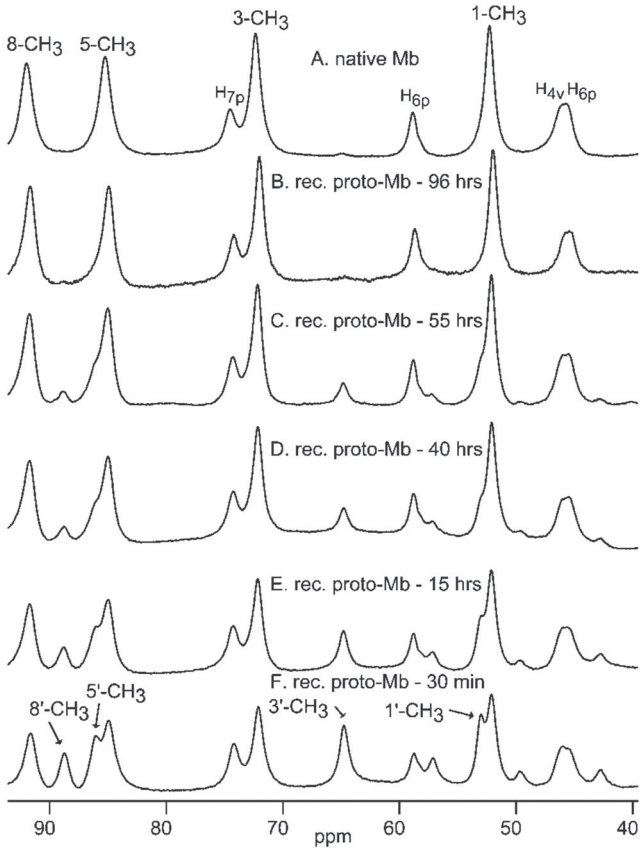

FIGURE 5 Reconstitution of Mb with protoheme as followed by nuclear magnetic resonance (NMR). From Rwere et al.[41]

one of the vinyl groups is less conjugated. An upshift from 408 to 422 cm^{-1}, as observed in the low wavenumber region, was tentatively assigned to a bending vibration associated to the change of the torsional angle of a vinyl group, in agreement with the variations observed in the high wavenumber region. However, as explained by the authors, the precise assignment of this band to a specific vinyl group of the reversed conformer would have required selective methyl or vinyl group deuteration. Accordingly, Mie et al. observed that only the vinyl bending modes in the low-wavenumber region notably differed in Mb reconstituted with symmetric protoheme isomers, thereby reflecting altered heme peripheral contacts.[14] Similar results were also confirmed for the reversed conformation in the ferrous CO and ferric cyanide complexes of deoxyMb. However, it is worth noting that the heme orientation did not change either the ν (Fe-Im) stretching vibration between the Fe atom and fifth histidyl imidazole ligand or the vibrations between the Fe atom and the distal CO and CN ligands.[40]

Recently, Kincaid and coworkers reconstituted Mb with protoheme deuterated only at the C_b position of the 4-vinyl group (Figures 1 and 3) and proved that the above mentioned upshift is due the 4-vinyl group, which in the reversed conformation assumes a position that is more out-of-plane than the newly positioned 2-vinyl group. This finding explains the wavenumber changes of the

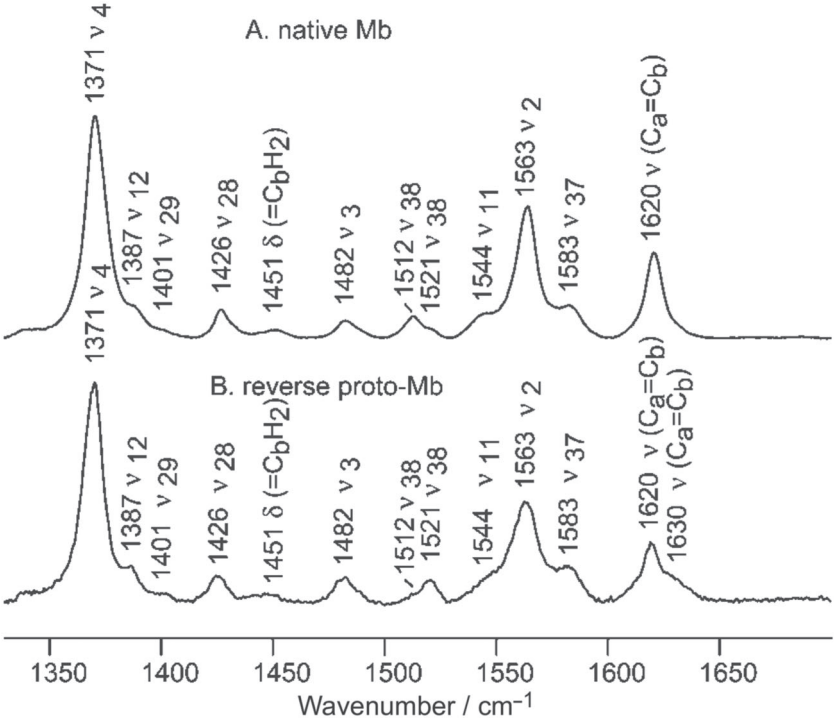

FIGURE 6 Comparison of the high wavenumber resonance Raman (RR) spectra of native Mb (canonical conformer) and the extracted spectra of the reversed conformation. Adapted from Rwere et al.[41]

vinyl modes between the native and the reversed conformation observed in the RR spectra of ferric, ferrous and its complex with CO, reported in Table 1.

Similarly, deoxy Hb A and deoxy rHb A, containing respectively the canonical and the reversed isomers, were studied by RR spectroscopy.[47] In the high wavenumber region, the RR bands were found to be similar between the two isomers, except for an upshift of the ν(C=C) vinyl stretching modes from 1619 to 1621 cm^{-1} upon changing the canonical to the reversed form, indicating that the in-plane skeletal vibrations of the heme are hardly affected by the orientational disorder. In the low wavenumber region, the authors showed that the bending modes of both propionate and vinyl groups are markedly different for the reversed heme with the respect to the canonical form. In fact, vinyl bending modes in Hb at 403 and 429 cm^{-1} merge into one band at 418 cm^{-1} in rHb A, whereas the single band of the propionyl bending modes at 364 cm^{-1} in the canonical isomer splits into two bands at 364 and 374 cm^{-1} in the reversed form. No change in the ν(Fe-His) mode was observed, which suggests a distortion of the heme peripheral groups of rHb A with the reversed form. Such distortion must involve only the peripheral groups, as no differences in the ν_8 and γ_7 modes were observed in the two isomers, showing that the heme planarity is maintained. Therefore, also the observed upshift of the ν(C=C) mode in the reversed form with respect to the canonical case is caused by a change in the vinyl side chain orientation. In rHb A mutants, no reversed heme conformer was detected.

Furthermore, the Fe-CO stretching mode band at 505 cm^{-1} and the Fe-C-O bending mode at 581 cm^{-1} in their CO complexes did not display any differences, while distinct relative intensities changes of the vinyl stretching modes observed at about 1620 and 1630 cm^{-1} were observed between the two conformers. Similar changes in the RR bands of the side chains were observed upon ligand dissociation.

New insights for the identification of rotational heme disorder in heme proteins have been provided recently by the combination of solution RR spectroscopy using polarized light different excitation wavelengths, and single crystal micro-RR spectroscopy, together with crystal structures of murine wild-type (WT) Ngb and selected variants.[5,43]

The structural heterogeneity of WT murine Ngb has been clearly detected by the solution ^{1}H-NMR spectrum[35] and in the 1.5 Å-resolution X-ray structure[4] of the ferric form (Figure 7). Two different 6-coordinated low spin conformers mutually rotated by 180° about the α,γ-*meso* axis have been identified, where the reversed insertion represents the main conformer with about 70% occupancy. The double heme insertion is a feature that arises from the expanded heme crevice necessary to allow heme sliding upon ligand binding.[4,89,90] Moreover, the structure revealed that the heme group is almost planar in the reversed form (Table 2, reversed), but distorted in the canonical form (Table 2, canonical). Since a planar heme configuration should have a smaller core size with respect to a distorted one, RR core size marker band wavenumbers, being inversely correlated with the size of the porphyrin core, are expected to differ.

Solution and *in crystallo* RR spectra of ferric WT Ngb and selected mutants were almost identical (Figure 8), indicating that the heme geometry and orientation are not affected by the crystal lattice.

The spectra obtained with two different excitation wavelengths and in polarized light (Figure 9) showed the presence of a double set of core-size markers bands in agreement with the presence of two conformers, both characteristic of a bis-His 6-coordinate low spin heme, due to both the distal (His64) and proximal histidines (His96) being coordinated to the heme iron (Figure 1). Therefore, the species with a smaller core (the reversed conformer) has been identified with the set of bands showing higher wavenumbers than the one assigned to the canonical insertion. Moreover, marked changes were expected in the vinyl stretching region due to the different disposition of the peripheral vinyl groups in the two conformers. Among the four vinyl stretching modes (two for each heme), only two vinyl stretching bands were identified in the high wavenumber region, at 1620 and

TABLE 1 Wavenumbers of the vinyl stretching and bending modes in the canonical and reversed conformations of ferric, ferrous, and CO complex of Mb

	Canonical form			Reversed form		
Mode	**Fe (II)**	**FeII (CO)**	**Fe (III)**	**Fe (II)**	**FeII (CO)**	**Fe (III)**
δ($C_\beta C_a C_b$) (2)	405	412	408	436	438	439
δ($C_\beta C_a C_b$) (4)	436	438	439	420	427	422
ν(C=C) (2)	1618	1619	1620	1618	1619	1620
ν(C=C) (4)	1618	1619	1620	1630	1628	1630

Note: Adapted from Rwere et al.[42]

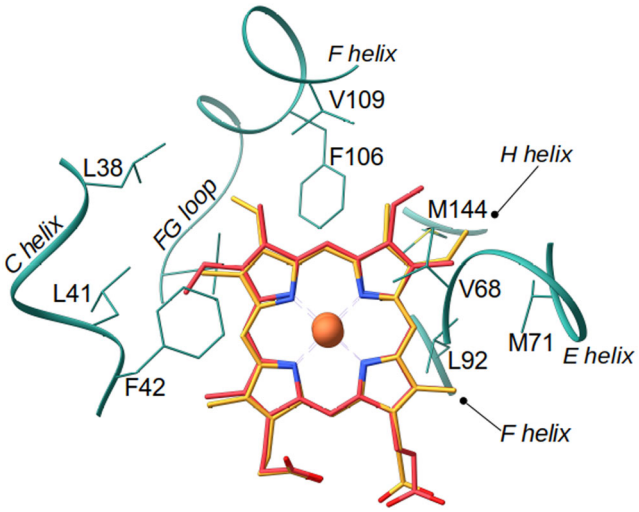

FIGURE 7 Double heme insertion in murine WT neuroglobin (1Q1F). The reversed and canonical heme conformers are reported in yellow and red, respectively. Top view from distal His64. The two heme conformers are related by the indicated 180° rotation about the α,γ–meso axis of the heme plane. Residues surrounding the vinyl groups (distance ≤ 4 Å) are shown as green sticks. From Exertier et al.[5] [Colour figure can be viewed at wileyonlinelibrary.com]

TABLE 2 Fe-N_{H96} (proximal) and Fe- N_{H64} (distal) distances (Å) and the His64-Fe-His96 angles of WT murine Ngb in its reversed and canonical conformers

	WT	
	Reversed	**Canonical**
Fe-His64 (distal) (Å)	1.9	2.1
Fe-His96 (proximal) (Å)	2.2	1.9
His64-Fe-His96 angle (°)	177	156

Note: From Vallone et al.[4]

1631 cm^{-1} (Figure 9), whereas three $\delta(C_\beta C_a C_b)$ bending modes at 404, 416, and 428 cm^{-1} were assigned in the low wavenumber region (Figure 10).

Based on the correlation between the torsional angles and the vinyl stretching wavenumbers, it has been concluded that in Ngb, both in the solution and crystalline forms, the reversed conformer is in the cis conformation ($\tau = 32.05°$ and 27.39° for vinyl 2 and 4, respectively) characterized by ν(C=C) stretching and $\delta(C_\beta C_a C_b)$ bending modes at 1631 cm^{-1} and 428 cm^{-1}, respectively (Table 4). Hence, similar to the case of reversed Mb, the Ngb vinyl substituent in position 4 changes its conformation from the trans to cis arrangement, while the conformation of the vinyl group in position 2 remains unchanged. The torsional angles (τ) of the vinyl groups for the two conformers of WT Ngb are reported in Table 4, together with those related to the canonical and reversed conformers of Mb.[42]

To gain a better understanding of the contributions of the overlapped vibrations in the 1600–1700 cm^{-1} region, Milazzo and coworkers compared the RR spectra of murine Ngb WT and the Gly-loop$^{44–47}$/F106A mutant (Figure 11).[43] This mutant, which contains both the mutation of the CDloop (Gly-loop), conferring an enhanced flexibility to the protein, and the F106A mutation, was studied to probe the role of heme sliding in the internal cavity and the function of the CD loop in controlling ligand affinity.[5]

By a refined curve fitting analysis, two distinct ν_{10} bands were found and assigned to the two conformers with different relative intensities for the murine Ngb Gly-loop$^{44–47}$/F106A mutant and the WT in the ferric form. Concomitantly, three ν(C=C) vinyl stretching modes were also observed in the high wavenumber region at 1620, 1629, and 1631 cm^{-1}. The intensity of the mode at 1629 cm^{-1} increases in the mutant, where the canonical form is predominant, at the expense of that at 1631 cm^{-1}, in agreement with the assignment in Table 4. Interestingly, the $\delta(C_\beta C_a C_b)$ vinyl bending modes in the low wavenumber region spectra show a similar trend for the mutant with an increase of the band at 416 cm^{-1}, related to the vinyl in position 2 of the canonical isomer (Figure 10).

The possibility to identify the marker bands for each conformer has given clear evidence that the Gly-loop$^{44–47}$/F106A mutation alters the equilibrium between the two conformers with an increase of the canonical conformer at the expense of the reversed form. This analysis of the RR results is in complete agreement with the crystal structure. In fact, in the Gly-loop$^{44–47}$/F106A mutant, Phe106 is in contact with the vinyl group in position 4 in the reversed conformer. The Gly-loop mutation, i.e. the introduction of a GGG sequence within the CD loop, leads to a lifting of the CD corner, therefore, releasing the steric hindrance imposed on this vinyl substituent, and resulting in a change of conformation from cis to trans that favors an increase of the canonical conformer population.

6 | CONCLUSION

Reconstitution of heme proteins with hemins may give rise to two conformers, which differ in the orientation of the heme group by a 180° rotation about the α,γ-meso axis in the heme pocket, called reversed and canonical hemes, respectively. However, the two isomers have been

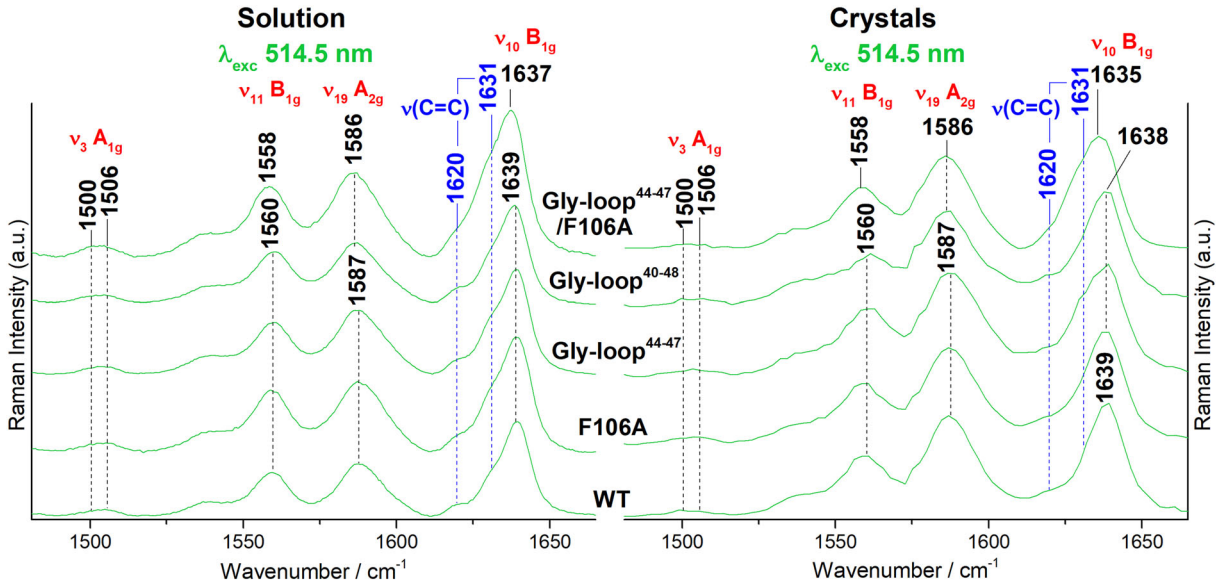

FIGURE 8 Comparison of the high wavenumber region resonance Raman (RR) spectra in solution and crystal states of WT murine Ngb and selected variants obtained with 514.5 nm excitation. Comparison of the experimental conditions is reported in Table 3. From Milazzo et al.[43] [Colour figure can be viewed at wileyonlinelibrary.com]

TABLE 3 Comparison of the experimental conditions used for the macro- (M-RR) and micro-resonance Raman (m-RR) experiments on WT murine Ngb and selected variants

	Concentration		Laser power		Integration time (min)	
	M-RR	m-RR	M-RR	m-RR	M-RR	m-RR
WT	160 μM	1.7 mM	70 mW	1.8 mW	30	5
F106A	180 μM	900 μM	70 mW	1.8 mW	68	30
Gly-loop$^{44–47}$	180 μM	540 μM	70 mW	1.8 mW	60	30
Gly-loop$^{40–48}$	180 μM	1 mM	70 mW	1.8 mW	125	10
Gly-loop$^{44–47}$/F106A	120 μM	120 μM	70 mW	1.8 mW	30	50

Note: From Milazzo et al.[43]

observed also in native proteins. Heme orientation can affect the activity and the functional properties of the protein and it is essential to have tools able to highlight this structural motif. In addition to X-ray crystallography, also CD, NMR, and RR spectroscopies have been found to be particularly informative.

While distinct CD signals were found to be dependent on both the heme planarity and the side chain orientation of the two conformers providing qualitative information, NMR can detect quantitatively heme heterogeneity and its time-dependent interconversion process in solution and in crystals. Furthermore, it has been shown that the interactions of the heme peripheral substituents with the residues of the protein pocket have a crucial role in determining the preferential heme orientation, but the mechanism of heme rotation is not thoroughly understood yet.

More recently, RR has been applied to elucidate the specific spectral changes associated with heme orientational disorder, as the vibrational modes of the heme can be selectively intensified by the resonance conditions. In addition, this technique can be applied to both crystals and solutions, using reduced concentrations and volumes, as compared to NMR. The modes associated with the heme peripheral vinyl groups were found to be affected by the heme isomerism, as also observed by NMR. A peculiar case is represented by the recent study on murine neuroglobin, a 6-coordinate low spin heme

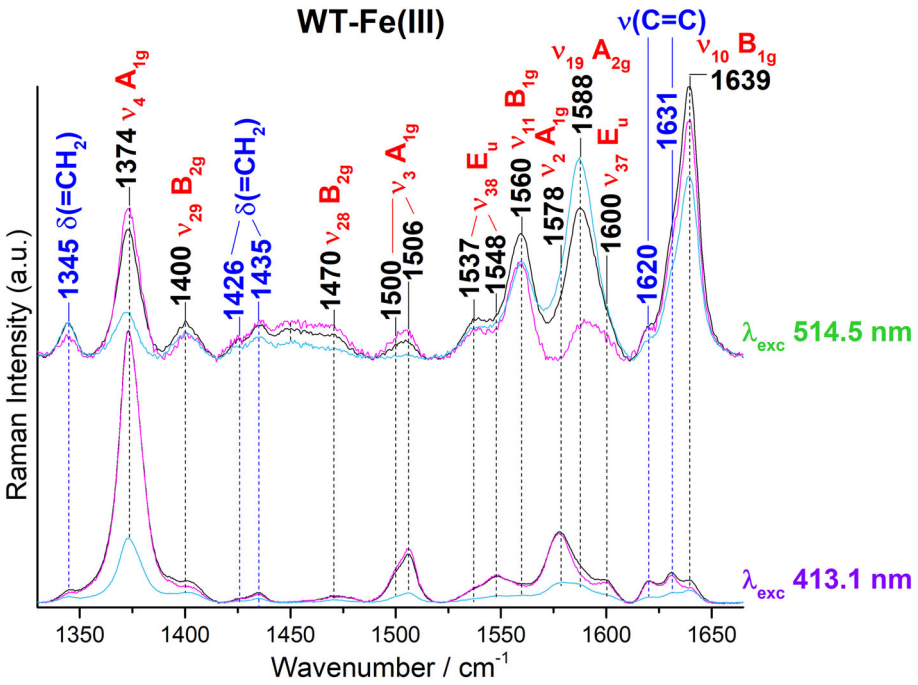

FIGURE 9 Resonance Raman (RR) spectra in polarized light of WT murine Ngb in solution taken with two different excitation wavelengths. Nonpolarized (black traces), parallel polarized (pink traces), and perpendicularly polarized (light blue traces) high wavenumber region RR spectra. Adapted from Milazzo et al.[43] [Colour figure can be viewed at wileyonlinelibrary.com]

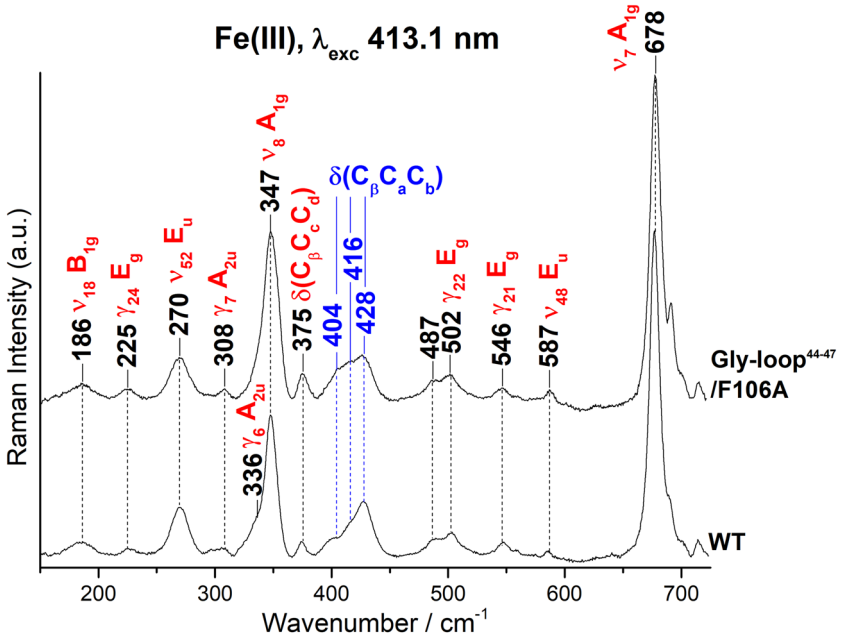

FIGURE 10 Low wavenumber region resonance Raman (RR) spectra of ferric murine Ngb WT (bottom) and the Gly-loop$^{44–47}$/F106A mutant (top), in solution, taken with a 413.1 nm excitation. Adapted from Milazzo et al.[43] [Colour figure can be viewed at wileyonlinelibrary.com]

protein displaying both the canonical and reversed heme orientations. Interestingly, The X-ray data showed that the two conformers are structurally different. The heme group is almost planar in the reversed form but distorted in the canonical form. Accordingly, the reversed and canonical heme conformers, both in the crystal and solution states, gave rise to two distinct sets of RR vibrational modes, since the core size marker band wavenumbers of the two conformers are inversely correlated with the size of the porphyrin core. Moreover, a correlation has been found between the stretching wavenumber and the cis/trans conformations of the vinyl groups of the reversed and canonical isomers. Therefore, the combination of RR spectroscopy on single crystal and solution samples has proved to be a sensitive diagnostic tool that could be extended to other heme proteins to detect heme

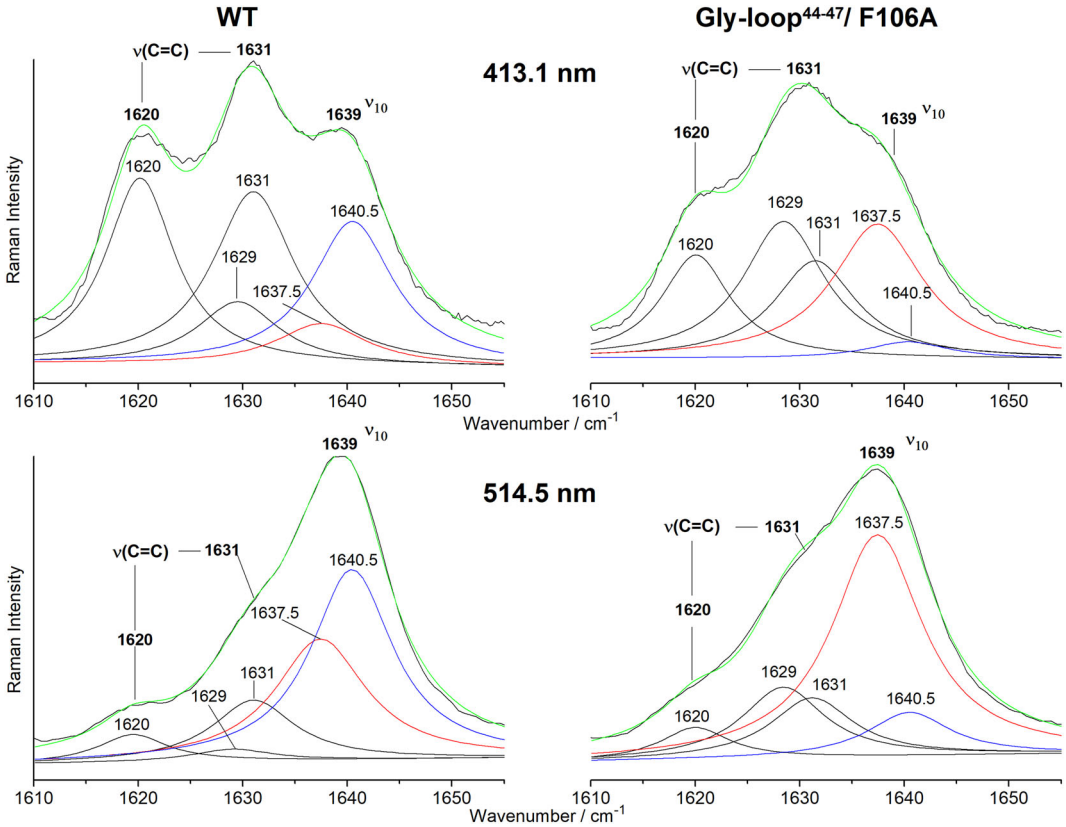

FIGURE 11 Curve-fitting analysis of the ν(C=C)/ν_{10} bands region of murine Ngb WT and the Gly-Loop$^{44–47}$/F106A mutant in solution. Resonance Raman (RR) spectra of the WT (left) and Gly-Loop$^{44–47}$/F106A mutant (right) have been obtained with 413 nm (top) and 514.5 nm (bottom) excitation wavelengths. The bands related to the reversed and canonical heme conformers are reported in blue and red, respectively. Bandwidths are 8.0, 9.5, 9.5, 10.5, and 9.5 cm^{-1} for the bands at 1620, 1629, and 1631 [ν(C=C)], 1637.5 (ν_{10}), and 1640.5 cm^{-1} (ν_{10}), respectively. In fact, in the spectra obtained with 514.5-nm excitation the ν(C=C) stretching modes of the two vinyl substituents are expected to be absent or very weak. RR spectra from Milazzo et al.[43] The analysis was performed using a spectral simulation program (LabCalc; Fisher Scientific Company L.L.C., Pittsburg, PA, USA) with a Lorentzian line shape to determine the peak positions, bandwidths, and intensities [Colour figure can be viewed at wileyonlinelibrary.com]

TABLE 4 Vinyl orientations (*cis* and *trans*), torsion angles (τ) and the corresponding RR stretching and bending wavenumbers (cm^{-1})[43] of the canonical and reversed conformers of ferric WT murine Ngb (1Q1F)[4] together with the canonical[66] and reversed[42] conformers of ferric Mb (from horse heart) for comparison

	WT murine Ngb canonical		**WT murine Ngb reversed**		**Horse heart Mb reversed**		**Horse heart Mb canonical**	
Vinyl position	**2**	**4**	**2**	**4**	**2**	**4**	**2**	**4**
Orientation	cis	**trans**	cis	**cis**	trans	**cis**	trans	**trans**
τ (°)	23.34	**−173.6**	32.05	**27.39**		**40–75**	−97.8	**−134.0**
ν(C=C) exp.	1631	**1620**	1631	**1631**	1620	**1630**	1620	**1620**
ν(C=C) calc.	*1629*	***1620***	*1631*	***1630***		***1632–1629***	*1623*	***1615***
$\delta(C_\beta C_a C_b)$	416	**404**	428	**428**	422	**439**	439	**408**

Note: The calculated wavenumbers (in italics) of the stretching vibrations of Ngb[43] and Mb[66] according to Marzocchi and Smulevich[71] are also reported.

orientational disorder, even in the absence of structural data.

ACKNOWLEDGEMENTS

F.S. was the recipient of a fellowship partially funded by MIUR-Italy ("Progetto Dipartimenti di Eccellenza 2018-2022" allocated to Department of Chemistry "Ugo Schiff").

ORCID

Cécile Exertier https://orcid.org/0000-0001-7457-6895
Maurizio Becucci https://orcid.org/0000-0002-2428-471X
Giulietta Smulevich https://orcid.org/0000-0003-3021-8919

REFERENCES

[1] T. Jue, R. Krishnamoorthi, G. N. La Mar, *J. Am. Chem. Soc.* **1983**, *105*, 5701.
[2] G. N. La Mar, N. L. Davis, D. W. Parish, K. M. Smith, *J. Mol. Biol.* **1983**, *168*, 887.
[3] T. Hayashi, in *Handbook of Porphyrin Science* (Eds: K. M. Kadish, K. M. Smith, R. Guillard), World Scientific, Singapore **2010**, 1.
[4] B. Vallone, K. Nienhaus, M. Brunori, G. U. Nienhaus, *Proteins* **2004**, *56*, 85.
[5] C. Exertier, L. Milazzo, I. Freda, L. C. Montemiglio, A. Scaglione, G. Cerutti, G. Parisi, M. Anselmi, G. Smulevich, C. Savino, B. Vallone, *Sci. Rep.* **2019**, *9*, 1.
[6] G. N. La Mar, Y. Yamamoto, T. Jue, K. M. Smith, R. K. Pandey, *Biochemistry* **1985**, *24*, 3826.
[7] Y. Yamamoto, G. N. La Mar, *Biochemistry* **1986**, *25*, 5288.
[8] G. N. La Mar, W. S. Smith, N. L. Davis, D. L. Budd, M. J. Levy, *Biochem. Biophys. Res. Commun.* **1989**, *158*, 462.
[9] R. Santucci, F. Ascoli, G. N. La Mar, R. K. Pandey, K. M. Smith, *Biochim. Biophys. Acta- Protein Struct. Mol.* **1993**, *1164*, 133.
[10] G. N. La Mar, J. D. Satterlee, J. S. De Roop, in *The Porphyrin Handbook* (Eds: K. M. Kadish, K. M. Smith, M. Guilard) Vol. 5, Academic Press, San Diego **2000**, 185.
[11] G. N. la Mar, D. L. Budd, D. B. Viscio, K. M. Smith, K. C. Langry, *Proc. Natl. Acad. Sci. U. S. a.* **1978**, *75*, 5755.
[12] G. N. La Mar, R. Krishnamoorthi, H. Toi, *J. Am. Chem. Soc.* **1984**, *106*, 6395.
[13] G. N. La Mar, U. Pande, J. B. Hauksson, R. K. Pandey, K. M. Smith, *J. Am. Chem. Soc.* **1989**, *111*, 485.
[14] Y. Mie, C. Yamada, G. P. J. Hareau, S. Neya, T. Uno, N. Funasaki, K. Nishiyama, I. Taniguchi, *Biochemistry* **2004**, *43*, 13149.
[15] C. Kiefl, N. Sreerama, R. Haddad, L. Sun, W. Jentzen, Y. Lu, Y. Qiu, J. A. Shelnutt, R. W. Woody, *J. Am. Chem. Soc.* **2002**, *124*, 3385.
[16] A. Bocahut, V. Derrien, S. Bernad, P. Sebban, S. Sacquin-Mora, E. Guittet, E. Lescop, *J. Biol. Inorg. Chem.* **2013**, *18*, 111.
[17] L. Yang, Y. Ling, Y. Zhang, *J. Am. Chem. Soc.* **2011**, *133*, 13814.
[18] H. S. Aojula, M. T. Wilson, A. Drake, *Biochem. J.* **1986**, *237*, 613.
[19] A. Bellelli, R. Foon, F. Ascoli, M. Brunori, *Biochem. J.* **1987**, *246*, 787.
[20] R. Santucci, J. Mintorovitch, I. Constantinidis, J. D. Satterlee, F. Ascoli, *Biochim. Biophys. Acta- Protein Struct. Mol.* **1988**, *953*, 201.
[21] B. D. Howes, S. Helbo, A. Fago, G. Smulevich, *J. Inorg. Biochem.* **2012**, *109*, 1.
[22] K. Gersonde, H. Sick, M. Overkamp, K. M. Smith, D. W. Parish, *Eur. J. Biochem.* **1986**, *157*, 393.
[23] F. A. Walker, D. Emrick, J. E. Rivera, B. J. Hanquet, D. H. Buttlaire, *J. Am. Chem. Soc.* **1988**, *110*, 6234.
[24] Y. Yamamoto, T. Nakashima, E. Kawano, R. Chûjô, *Biochim. Biophys. Acta - Protein Struct. Mol. Enzymol.* **1998**, *1388*, 349.
[25] M. Nagai, Y. Nagai, Y. Aki, K. Imai, Y. Wada, S. Nagatomo, Y. Yamamoto, *Biochemistry* **2008**, *47*, 517.
[26] C. Moczygemba, J. Guidry, P. Wittung-Stafshede, *FEBS Lett.* **2000**, *470*, 203.
[27] D. Peng, J. D. Satterlee, L.-H. H. Ma, J. L. Dallas, K. M. Smith, X. Zhang, M. Sato, G. N. La Mar, *Biochemistry* **2011**, *50*, 8823.
[28] J. Wojaczyński, H. Wójtowicz, M. Bielecki, M. Olczak, J. W. Smalley, L. Latos-Grażyński, T. Olczak, *Biochem. Biophys. Res. Commun.* **2011**, *411*, 299.
[29] F. Yang, H. Zhang, M. Knipp, *Biochemistry* **2009**, *48*, 235.
[30] S. Juillard, S. Chevance, A. Bondon, G. Simonneaux, *Biochim. Biophys. Acta - Proteins Proteomics* **2011**, *1814*, 1188.
[31] M. J. Cocco, S. V. Taylor, J. T. J. Lecomte, D. Barrick, *J. Am. Chem. Soc.* **1992**, *114*, 11000.
[32] M. C. Piro, V. Militello, M. Leone, Z. Gryczynski, S. V. Smith, W. S. Brinigar, A. Cupane, F. K. Friedman, C. Fronticelli, *Biochemistry* **2001**, *40*, 11841.
[33] T. Burmester, B. Welch, S. Reinhardt, T. Hankeln, *Nature* **2000**, *407*, 520.
[34] A. Fabrizius, D. Andre, T. Laufs, A. Bicker, S. Reuss, E. Porto, T. Burmester, T. Hankeln, *Neuroscience* **2016**, *337*, 339.
[35] W. Du, R. Syvitski, S. Dewilde, L. Moens, G. N. La Mar, *J. Am. Chem. Soc.* **2003**, *125*, 8080.
[36] A. Pesce, S. Dewilde, M. Nardini, L. Moens, P. Ascenzi, T. Hankeln, T. Burmester, M. Bolognesi, *Structure* **2003**, *11*, 1087.
[37] A. Fago, A. J. Mathews, S. Dewilde, L. Moens, T. Brittain, *J. Inorg. Biochem.* **2006**, *100*, 1339.
[38] H. S. Aojula, M. T. Wilson, G. R. Moore, D. J. Williamson, *Biochem. J.* **1988**, *250*, 853.
[39] R. Santucci, F. Ascoli, G. N. La Mar, D. W. Parish, K. M. Smith, *Biophys. Chem.* **1990**, *37*, 251.
[40] F. Rwere, P. J. Mak, J. R. Kincaid, *Biochemistry* **2008**, *47*, 12869.
[41] F. Rwere, P. J. Mak, J. R. Kincaid, *Biopolymers* **2008**, *89*, 179.
[42] F. Rwere, P. J. Mak, J. R. Kincaid, *J. Raman. Spectrosc.* **2014**, *45*, 97.
[43] L. Milazzo, C. Exertier, M. Becucci, I. Freda, L. C. Montemiglio, C. Savino, B. Vallone, G. Smulevich, *Febs j.* **2020**, *287*, 4082.
[44] M. C. Hsu, R. W. Woody, *J. Am. Chem. Soc.* **1971**, *93*, 3515.
[45] W. R. Light, R. J. Rohlfso, G. Palmern, J. S. Olson, *J. Biol. Chem.* **1987**, *262*, 46.
[46] R. W. Woody, G. Pescitelli, *Z. Naturforsch.* **2014**, *69*, 313.

[47] M. Nagai, N. Mizusawa, T. Kitagawa, S. Nagatomo, *Biophys. Rev.* **2018**, *10*, 271.
[48] M. Nagai, C. Kobayashi, Y. Nagai, K. Imai, N. Mizusawa, H. Sakurai, S. Neya, M. Kayanuma, M. Shoji, S. Nagatomo, *J. Phys. Chem. B* **2015**, *119*, 1275.
[49] M. Nagai, Y. Nagai, Y. Aki, H. Sakurai, N. Mizusawa, T. Ogura, T. Kitagawa, Y. Yamamoto, S. Nagatomo, *Chirality* **2016**, *28*, 585.
[50] S. Yee, D. H. Peyton, *FEBS Lett.* **1991**, *290*, 119.
[51] G. N. La Mar, J. S. de Ropp, K. M. Smith, K. C. Langry, *J. Am. Chem. Soc.* **1980**, *102*, 4833.
[52] G. N. La Mar, P. D. Burns, J. T. Jackson, K. M. Smith, K. C. Langry, P. Strittmatter, *J. Biol. Chem.* **1981**, *256*, 6075.
[53] S. Neya, N. Funasaki, *Biochemistry* **1986**, *25*, 1221.
[54] J. B. Hauksson, G. N. La Mar, R. K. Pandey, I. N. Rezzano, K. M. Smith, *J. Am. Chem. Soc.* **1990**, *112*, 6198.
[55] Y. Kanai, A. Harada, T. Shibata, R. Nishimura, K. Namiki, M. Watanabe, S. Nakamura, F. Yumoto, T. Senda, A. Suzuki, S. Neya, Y. Yamamoto, *Biochemistry* **2017**, *56*, 4500.
[56] H. Ishikawa, S. Takahashi, K. Ishimori, I. Morishima, *Biochem. Biophys. Res. Commun.* **2004**, *324*, 1095.
[57] C. L. Hunter, E. Lloyd, L. D. Eltis, S. P. Rafferty, H. Lee, M. Smith, A. G. Mauk, *Biochemistry* **1997**, *36*, 1010.
[58] M. D. Altose, Y. Zheng, J. Dong, B. A. Palfey, P. R. Carey, *Proc. Natl. Acad. Sci. U. S. A.* **2001**, *98*, 3006.
[59] G. Smulevich, Y. Wang, S. L. Edwards, T. L. Poulos, A. M. English, T. G. Spiro, *Biochemistry* **1990**, *29*, 2586.
[60] G. Smulevich, Y. Wang, T. G. Spiro, J. M. Mauro, L. A. Fishel, J. Kraut, J. Wang, *Biochemistry* **1990**, *29*, 7174.
[61] G. Smulevich, T. G. Spiro, *Methods Enzymol.* **1993**, *226*, 397.
[62] G. Smulevich, *J. Porphyr. Phthalocyanines* **2019**, *23*, 691.
[63] T. G. Spiro, X. Li, in *Biological Applications of Raman Spectroscopy* (Ed: T. G. Spiro), Wiley, USA **1988**, 1.
[64] M. Gouterman, *The Porphyrins*, Academic Press, New York **1978**, 1.
[65] T. G. Spiro, *Adv. Protein Chem.* **1985**, *37*, 111.
[66] J. R. Kincaid, in *The Porphyrin Handbook* (Eds: K. M. Kadish, K. M. Smith, M. Guilard) Vol. 7, Academic Press, San Diego **1999**, 225.
[67] T. G. Spiro, T. C. Strekas, *J. Am. Chem. Soc.* **1974**, *96*, 338.
[68] J. Tang, A. C. Albrecht, *Raman Spectroscopy*, Springer, US **1970**, 33.
[69] K. Uchida, Y. Susai, E. Hirotani, T. Kimura, T. Yoneya, H. Takeuchi, I. Harada, *J. Biochem.* **1988**, *103*, 979.
[70] G. Smulevich, S. Hu, K. R. Rodgers, D. B. Goodin, K. M. Smith, T. G. Spiro, *Biospectroscopy* **1996**, *2*, 365.
[71] M. P. Marzocchi, G. Smulevich, J. Raman, *Spectrosc.* **2003**, *34*, 725.
[72] S. Choi, T. G. Spiro, K. C. Langry, K. M. Smith, D. L. Budd, G. N. L. Mar, *J. Am. Chem. Soc.* **1982**, *104*, 4345.
[73] G. T. Babcock, W. R. Widger, W. A. Cramer, W. A. Oertling, J. G. Metz, *Biochemistry* **1985**, *24*, 3638.
[74] J. K. Hurst, T. M. Loehr, J. T. Curnutte, H. Rosen, *J. Biol. Chem.* **1991**, *266*, 1627.
[75] J. Hudeček, P. Hodek, E. Anzenbacherová, P. Anzenbacher, *Biochim. Biophys. Acta* **2007**, *1770*, 413.
[76] C. Jakopitsch, E. Droghetti, F. Schmuckenschlager, P. G. Furtmüller, G. Smulevich, C. Obinger, *J. Biol. Chem.* **2005**, *280*, 42411.
[77] E. Droghetti, B. D. Howes, A. Feis, P. Dominici, M. Fittipaldi, G. Smulevich, *J. Inorg. Biochem.* **2007**, *101*, 1812.
[78] F. P. Nicoletti, M. K. Thompson, B. D. Howes, S. Franzen, G. Smulevich, *Biochemistry* **2010**, *49*, 1903.
[79] B. Pal, K. Tanaka, S. Takenaka, T. Kitagawa, *J. Raman. Spectrosc.* **2010**, *41*, 1178.
[80] M. Ibrahim, E. R. Derbyshire, A. V. Soldatova, M. A. Marletta, T. G. Spiro, *Biochemistry* **2010**, *49*, 4864.
[81] P. J. Mak, M. C. Gregory, S. G. Sligar, J. R. Kincaid, *Biochemistry* **2014**, *53*, 90.
[82] A. I. Celis, B. R. Streit, G. C. Moraski, R. Kant, T. D. Lash, G. S. Lukat-Rodgers, K. R. Rodgers, J. L. DuBois, *Biochemistry* **2015**, *54*, 4022.
[83] L. Milazzo, T. Gabler, D. Pühringer, Z. Jandova, D. Maresch, H. Michlits, V. Pfanzagl, K. Djinović-Carugo, C. Oostenbrink, P. G. Furtmüller, C. Obinger, G. Smulevich, S. Hofbauer, *ACS Catal.* **2019**, *9*, 6766.
[84] D. Coppola, D. Giordano, L. Milazzo, B. D. Howes, P. Ascenzi, G. di Prisco, G. Smulevich, R. K. Poole, C. Verde, *Nitric Oxide: Biol. Chem.* **2018**, *73*, 39.
[85] S. Hofbauer, J. Helm, C. Obinger, K. Djinović-Carugo, P. G. Furtmüller, *Febs j.* **2020**, *287*, 2779.
[86] G. De Simone, A. Di Masi, G. M. Vita, F. Polticelli, A. Pesce, M. Nardini, M. Bolognesi, C. Ciaccio, M. Coletta, E. S. Turilli, M. Fasano, L. Tognaccini, G. Smulevich, S. Abbruzzetti, C. Viappiani, S. Bruno, P. Ascenzi, *Antioxid. Redox Sign.* **2020**, *33*, 229.
[87] C. M. Bianchetti, C. A. Bingman, G. N. Phillips, *Proteins* **2011**, *79*, 1337.
[88] S. Hu, K. M. Smith, T. G. Spiro, *J. Am. Chem. Soc.* **1996**, *118*, 12638.
[89] B. Vallone, K. Nienhaus, A. Matthes, M. Brunori, G. U. Nienhaus, *Proc. Natl. Acad. Sci. U. S. a.* **2004**, *101*, 17351.
[90] G. Avella, C. Ardiccioni, A. Scaglione, T. Moschetti, C. Rondinelli, L. C. Montemiglio, C. Savino, A. Giuffrè, M. Brunori, B. Vallone, *Acta Cryst. D* **2014**, *70*, 1640.

How to cite this article: Sebastiani F, Milazzo L, Exertier C, Becucci M, Smulevich G. Detecting rotational disorder in heme proteins: A comparison between resonance Raman spectroscopy, nuclear magnetic resonance, and circular dichroism. *J Raman Spectrosc*. 2021;1–14. https://doi.org/10.1002/jrs.6105